Thin scattering layers observed by airborne lidar

James H. Churnside and Percy L. Donaghay

Churnside, J. H., and Donaghay, P. L. 2009. Thin scattering layers observed by airborne lidar. – ICES Journal of Marine Science, 66: 778–789.

More than 2000 km of thin (<3 m) optical scattering layers were identified in 80 000 km of airborne lidar data collected from a variety of oceanic and coastal waters. The spatial characteristics of thin layers varied dramatically from (i) those that were self-contained features consistently <3–4 m thick over their 1–12 km extent to (ii) those that were clearly parts of much longer layers that had gaps and/or regions where the layer became more intense and much thicker than the 3-m criterion. The characteristics of the lidar signal suggest that plankton was the most likely source of scattering. Examples from upwelling regions, areas with large freshwater influx, and warm-core eddies are presented. The results are quite consistent with the characteristics observed in studies of thin plankton layers in fjords and near-coastal waters. These layers exhibit great spatial variability that is difficult to observe using traditional methods, and examples of layer perturbations by both linear and non-linear internal waves are presented. The results suggest that airborne lidar can be a powerful tool not only for detecting and mapping the spatial extent of thin scattering layers and linking their occurrence to larger scale physical processes, but also for tracking their evolution over time and guiding the ship-based sampling needed to understand their composition, dynamics, and impacts. Such a capability will be crucial in future studies designed to test the hypothesis that thin plankton layers have the spatial extent and intensity to play a key role in controlling the recruitment of fish larvae, biogeochemical cycling, trophic transfer processes, plankton biodiversity, and harmful algal bloom dynamics.

Keywords: internal waves, lidar, plankton layers, thin layers, upwelling.

Received 5 July 2008; accepted 25 January 2009; advance access publication 25 February 2009.

J. H. Churnside: NOAA Earth System Research Laboratory, 325 Broadway, Boulder, CO 80305, USA. P. L. Donaghay: Graduate School of Oceanography, University of Rhode Island, Narragansett, RI 02874, USA. Correspondence to J. H. Churnside: tel: +1 303 497 6744; fax: +1 303 497 5318; e-mail: james.h.churnside@noaa.gov.

Introduction

Although biological oceanographers have long recognized that plankton distributions can be patchy over an extremely wide range of scales (Cassie, 1963; Lasker, 1975; Mullin and Brooks, 1976), it was generally assumed that vertical mixing processes in the upper ocean were sufficiently intense to limit the persistence and spatial continuity/extent of patches thinner than a few metres. This assumption remained largely untested until instruments were developed that could simultaneously sample the physical, chemical, and biological structure of the water column down to scales of a few centimetres (Donaghay *et al.*, 1992; Hanson and Donaghay, 1998; Holliday *et al.*, 1998, 2003; Donaghay, 2004). Application of these high-resolution sampling techniques in topographically constrained systems (fjords) led to the discovery that plankton patches ranging in thickness from 10 cm to a few metres were, in fact, thin layers that could extend for kilometres and persist for days (Rines *et al.*, 2002) or even months (Sieburth and Donaghay, 1993; Johnson *et al.*, 1995). Equally important, these high-resolution sampling techniques demonstrated that these thin layers varied dramatically from surrounding waters both in concentration and species composition in ways that could affect the geochemical (Mason *et al.*, 1993; Scranton *et al.*, 1993, 1995; Sieburth and Donaghay, 1993; Hanson and Donaghay, 1998) and biological (Bjornsen and Nielsen, 1991; Donaghay *et al.*, 1992; Johnson *et al.*, 1995; Donaghay and Osborn, 1997; Cowles *et al.*, 1998; Holliday *et al.*, 2003; Donaghay, 2004) dynamics of the pelagic zone. Analysis of the acoustic and optical data collected during these studies indicates that differences in concentration and composition can be sufficiently large to affect the penetration and interpretation of acoustic (Holliday *et al.*, 2003) and optical (Petrenko *et al.*, 1998; Zaneveld and Pegau, 1998; Sullivan *et al.*, 2005) remote sensing techniques. However, analysis of a large set of simultaneous measurements of absorption, attenuation, and backscattering suggests that backscattering from some types of thin layer may be too weak to be detected remotely by lidar (Sullivan *et al.*, 2005).

Much of the detailed information about thin layers comes from intensive studies at a limited number of coastal sites. These include the multiyear studies of methane and mercury geochemical dynamics in the Pettaquamscutt Estuary, Rhode Island (Mason *et al.*, 1993; Scranton *et al.*, 1993, 1995; Sieburth and Donaghay, 1993), event-driven studies of highly toxic harmful algal blooms in European coastal waters (Nielsen *et al.*, 1990; Bjornsen and Nielsen, 1991), a series of instrument tests and initial process studies conducted over several years in East Sound, WA (Hanson and Donaghay, 1998; Dekshenieks *et al.*, 2001; Alldredge *et al.*, 2002; Rines *et al.*, 2002; McManus *et al.*, 2003), and studies of thin layer occurrence in open coastal waters off

Oregon (Cowles *et al.*, 1998) and California (Donaghay, 2004; McManus *et al.*, 2005; Sullivan *et al.*, 2005). Several of these studies resulted in a large enough body of temporal and spatial data on fine-scale physical and optical properties to allow a statistical analysis of the frequency of occurrence and properties of fine-scale layers and their association with fine-scale physical structures and processes (Dekshenieks *et al.*, 2001; Holliday *et al.*, 2003; Donaghay, 2004). For example, statistical analysis of 120 high-resolution (cm) vertical profiles collected in East Sound, WA, in 1995 showed that although fine-scale features <12 cm thick were rarely detected in subsequent profiles, fine-scale features that ranged in thickness from 12 cm to 3.6 m were in fact thin layers that were sufficiently extensive or spatially continuous to be detected in subsequent profiles. These thin layers had a maximum frequency of occurrence at a thickness of $\sim$1 m (Dekshenieks *et al.*, 2001; Holliday *et al.*, 2003; Donaghay, 2004). Such thin layers were observed in 54% of the profiles. Equally important, the analysis showed that thin layers could occur over a very wide range of density and velocity gradients as long as flow did not exceed the Richardson number criteria for turbulent flow.

Although those studies clearly demonstrated thin layers in coastal waters that were sufficiently intense to affect biogeochemical cycling, trophic transfer processes, and harmful algal bloom dynamics, they also raised a series of questions. First, what is the spatial extent and continuity of the thin layers, and how does it vary with environmental conditions? For example, do patterns of spatial extent and continuity differ between inshore and offshore environments? Do patterns of spatial extent differ between upwelling-favourable and -unfavourable conditions? Second, what is their frequency of occurrence, and how does it vary with environmental conditions? For example, does the frequency of occurrence vary between inshore and offshore environments? Are there general patterns of frequency of occurrence in systems with similar forcing (such as wind-driven upwelling vs. non-upwelling environments), or are the patterns highly site-specific? Third, are the above patterns of temporal and spatial occurrence consistent with thin-layer models (Franks, 1995; Donaghay and Osborn, 1997)? For example, do internal waves affect spatial continuity by creating gaps caused by internal wave mixing events? Fourth, do the thin plankton layers have sufficiently intense optical backscatter to be detected and mapped by optical remote sensing techniques such as lidar? If so, what are the limitations of existing systems, and can they be modified to address the above questions better?

Addressing these questions requires applying techniques such as airborne oceanographic lidar that can synoptically sample the fine-scale vertical structure in a variety of near-surface coastal and offshore oceanic environments. Synoptic sampling is particularly important in open waters to avoid the temporal–spatial confounding that is inherent in ship-based sampling (Platt and Denman, 1975). Oceanographic lidars use visible light, generally green, to investigate the upper ocean. Hoge *et al.* (1988) reported airborne lidar observations of scattering layers in the Northwest (NW) Atlantic. Vasilkov *et al.* (2001) observed layers in the same area using a polarized lidar. Churnside and Ostrovsky (2004) reported observations of a strong internal wave in the Gulf of Alaska by the perturbations of a scattering layer. However, none of those investigations was interested in the layer thickness.

The National Oceanic and Atmospheric Administration (NOAA) is developing an airborne lidar system for surveys of epipelagic fish (Churnside *et al.*, 1997, 2001) and zooplankton (Brown *et al.*, 2002; Churnside and Thorne, 2005), and has performed a number of experimental surveys in regions where stratification of the water column might be expected. The first flight tests of the system were over the Southern California Bight between 30 March and 21 April 1997 (Churnside *et al.*, 2001). Subsequent tests were made over the NW Atlantic along the coast of the Iberian Peninsula between 22 August and 9 September 1998 (Carrera *et al.*, 2006), over the Gulf of Alaska between 20 July and 10 September 2001 and between 11 May and 1 September 2002, over the Norwegian Sea between 15 and 23 July 2002, over the NE Pacific along the coast of Oregon and Washington between 9 and 17 July 2003, and over the Gulf of Alaska again between 20 July and 2 August 2003. Figure 1 is a chart of all the flight tracks included in the analysis. Data collected during winter (e.g. Churnside *et al.*, 2003) were not included in this study, because the stratification required for thin layers to form would not be expected in winter.

The lidar data were examined for the presence of thin scattering layers, defined as regions of enhanced lidar return whose full width at half maximum is <3 m and spatial extent exceeds 20 m. No minimum layer strength was included in this definition.

Except where noted, the dominant source of scattering in these layers was probably plankton. The polarization configuration that was used enhances the return from large (compared with

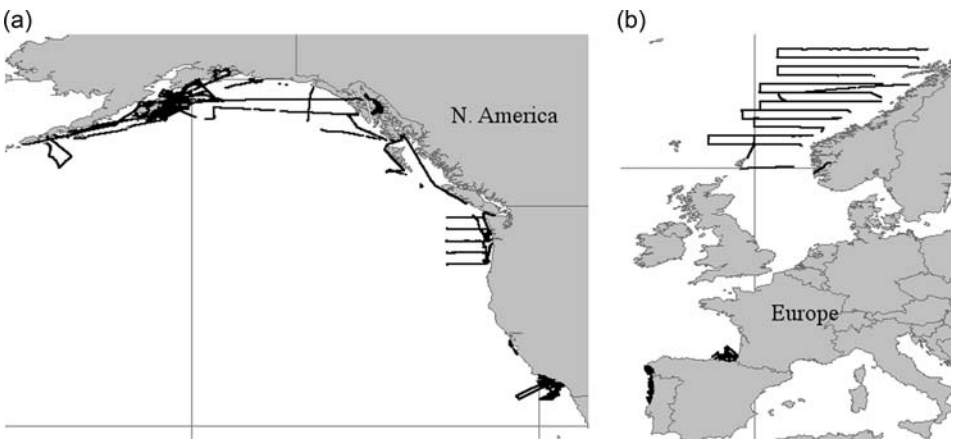

Figure 1. Chart showing all flight tracks used in the analysis as black lines: (a) Northeast Pacific, and (b) Northeast Atlantic.

wavelength) scattering particles of irregular shape. The techniques used to select plankton scattering from other sources have been demonstrated (Churnside and Thorne, 2005). Many of the data were collected in Case 1 waters, where the concentration of plankton is high compared with that of non-biogenic particles. Layers observed in Case 2 waters have similar spatial structures, suggesting similar scattering mechanisms. The spatial structures and optical properties observed are also consistent with those observed *in situ* and known to be plankton (Holliday *et al.*, 1998, 2003; Petrenko *et al.*, 1998; Rines *et al.*, 2002). For these reasons, although it is possible that some of the layers observed in inland waters might be composed of suspended sediments or marine snow (Alldredge *et al.*, 2002), it is unlikely. More work is needed to determine specific lidar signatures of thin-layer constituents.

Material and methods

The NOAA Fish Lidar, a non-scanning, profiling system (Churnside *et al.*, 2001), was used for all the surveys in this study. It transmitted 100 mJ of linearly polarized green (532 nm) light in a 12 ns pulse at a rate of 30 pulse s^{-1}. It was pointed 15° off nadir to minimize the specular reflection from the sea surface. The laser beam divergence was set so that the diameter of the laser spot on the surface was 5 m in the daytime. The 5-m spot is large enough that the power density at the surface is safe for humans (ANSI, 1993) and marine mammals (Zorn *et al.*, 2000). At the same time, it is small enough that the background sunlight is a small part of the overall signal. The scattered light from the water column was collected by a telescope with a field of view matched to the laser beam divergence. At night, background sunlight is not present, and the laser beam divergence and telescope field of view were expanded to produce a 15-m spot on the surface. This reduces the attenuation (Gordon, 1982), because more scattered photons contribute to the signal. The light collected by the telescope was detected by a photomultiplier tube, logarithmically amplified to increase the dynamic range, and digitized at a rate of 10^9 sample s^{-1}. The receiver was configured to detect linearly polarized light orthogonal to the transmitted plane of polarization to increase detectability (Lewis *et al.*, 1999).

Thin layers show up very clearly in a lidar signal (Figure 2a). The layer in this case was at a depth of 10–13 m off the shelf west of Oregon in 2003. The thickness of this layer was ~2 m, although there are several spots where it is as thick as 5 m. The black line at the top of the figure clearly shows where the thickness of the layer is less than the 3-m criterion. This layer, then, is not a continuous thin layer according to our definition, but a series of thin layers separated by regions that are thicker. The thicker regions are associated with regions where the layer extends up towards the surface. Figure 3, the profile of the first lidar shot of Figure 2a, shows both the raw lidar return and the return after processing to remove the effects of the uniform background scattering level and to correct for the attenuation of light in the water. The depth of the peak is 12.5 m, and the full width at half maximum is 1.7 m, both before and after processing. After deconvolution with the laser pulse shape, the estimated layer thickness is 1.1 m. The peak volume backscatter coefficient for this profile was 4.6×10^{-5} m^{-1} sr^{-1} (sr, steradian) compared with a maximum value of 7.7×10^{-5} m^{-1} sr^{-1} for the whole layer.

An additional layer is evident at the surface in the raw return. It has approximately the same strength as the deeper layer after correction for attenuation. In the processed data, this peak is removed. Sometimes, patchy scattering layers at the surface seemed to have scale sizes similar to visual observations of breaking waves; the scattering then was likely dominated by spray, foam, and bubbles associated with the breaking waves. Sometimes, a continuous scattering layer was observed to vary in depth, with parts of the layer reaching the surface; the scattering then was likely dominated by plankton that were following a density gradient or vertically migrating. The layers did not have the high-spatial-frequency components as did those associated with breaking waves, and tended to occur when no breaking waves were visible. Sometimes, we observed a surface layer that seemed to have characteristics of both scattering by breaking waves and scattering by plankton. Surface layers were also sometimes associated with regions of high turbidity, such as river plumes, although those tended to be thicker than the other surface layers observed. Because the scattering mechanism for surface layers cannot always be determined, surface layers were not included in this analysis.

The first step in the data analysis was a visual inspection of the original data files, which contain the logarithm of the raw lidar data. A list was made of those files that contained visible layers of any thickness, and these were subjected to further processing according to the following steps.

(i) First, the signal from ambient light was estimated by the average of the last 100 samples of each pulse, which was always after the returned laser light had decayed to negligible levels. Because the ambient light adds linearly to the laser signal, the estimated value was subtracted from each sample in the lidar return.

(ii) Next, a correction was applied for the range-squared geometric loss.

(iii) Then, the background scattering level and exponential attenuation were estimated using the signal from a depth of 2 m and the signal from a depth of 0.8 times the maximum penetration depth. The maximum penetration depth was defined as the depth at which the signal fell below a value that was 10 s.d. of the noise above the ambient light level. The upper value of 2 m was chosen to avoid the signals from breaking waves and foam that occur in some of the near-surface data. Those signals can extend to an apparent depth as great as 2 m under high-wind conditions, where the surface is rough within the illuminated area. An example of a profile through a surface layer can be seen in the raw data profile of Figure 3.

(iv) After that, the exponentially decaying background signal was subtracted from each profile, and the result was corrected for the measured attenuation. The result of this step in the data processing is illustrated by the heavy line in Figure 3.

(v) Next, the full width at half maximum for each peak in the data was measured, and a correction was applied to account for the finite laser pulse length. Because the return is a convolution of the layer profile and the laser pulse shape, the layer profile can be estimated by deconvolution. The layer thickness was estimated by the square root of the difference between the squares of the measured thickness and the 1.3-m length of the illumination. This works

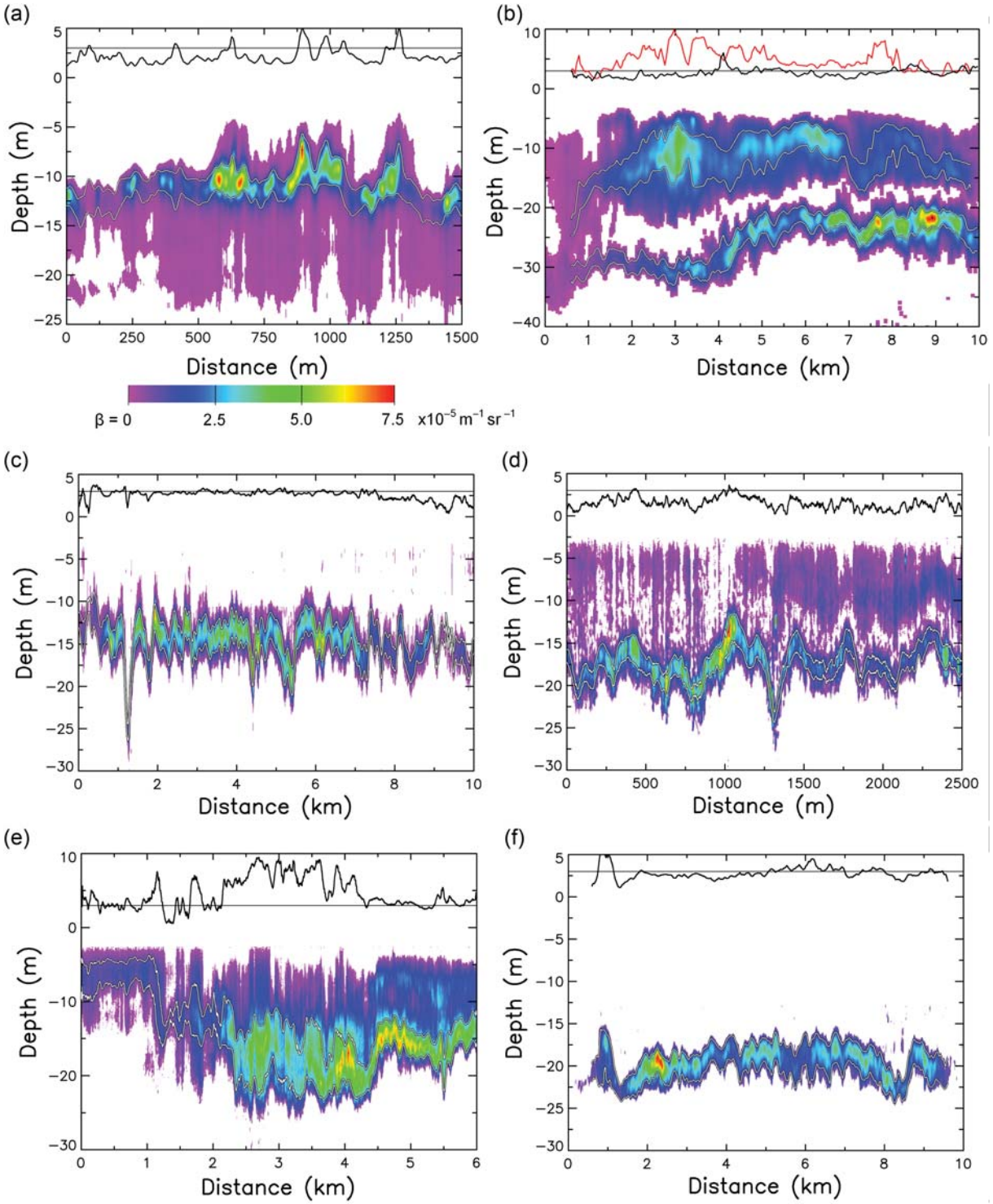

Figure 2. Vertical slices of lidar scattering layers. The white lines denote the half-power points above and below the peak. The thick black lines at the top are the layer thickness, and the thin line is 3 m. The colour bar has the same order for all panels, but the values apply to the first. (a) Transect off the Oregon shelf from 43.9894°N 127.8584°W to 43.9974°N 127.8415°W in water at a nearly constant depth of ∼2950 m. (b) Transect off the Washington shelf from 47.9887°N 127.9238°W to 47.9932°N 127.786°W in water at a nearly constant depth of 2610 m. The red line is the thickness of the upper layer. (c) Transect off Portugal from 41.1847°N 8.9506°W to 41.1010°N 8.9185°W in water 66 m deep. (d) Transect in the Gulf of Alaska from 56.7711°N 152.7488°W to 56.7778°N 152.7095°W in water 63 m deep. (e) Transect along the eastern edge of the Vøring Plateau in the Norwegian Sea from 64.9995°N 4.8535°E to 65.0000°N 4.7203°E in water ranging in depth from 821 m at the start to 877 m at the end. (f) Transect through a warm-core eddy in the Gulf of Alaska (western eddy; see Figure 6 later) from 53.4252°N 160.5397°W to 53.3339°N 160.4347°W in water ranging from ∼6100 m deep at the start to ∼5500 m deep at the end.

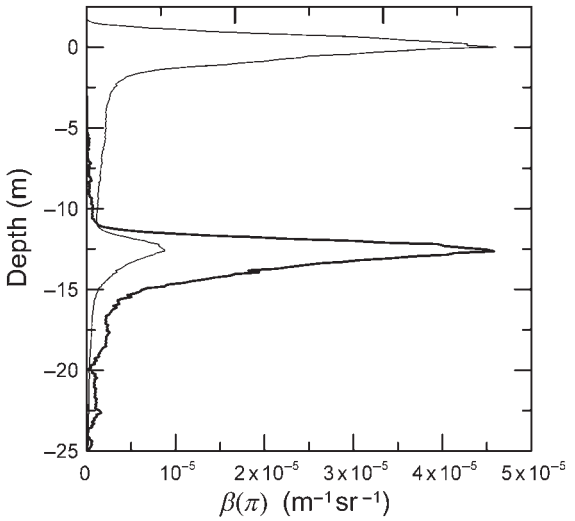

Figure 3. Single depth profile of volume backscatter coefficient $\beta(\pi)$ from the first lidar shot of Figure 2a. The thin line is the raw lidar return and the heavy line is the return after processing to remove the effects of the uniform background scattering level and to correct for the attenuation of light in the water. The full width at half maximum of the layer 12.5 m deep is 1.7 m in both the raw return and the processed return.

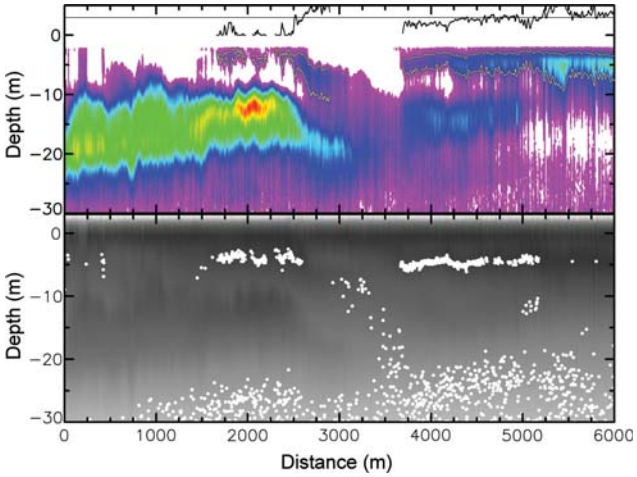

Figure 4. Vertical slice of raw lidar data along 6 km of flight track from off the Oregon shelf extending from 44.0106°N 127.732°W to 44.0093°N 127.8075°W in water ranging in depth from 2886 m at the start to 2955 m at the end of the transect. The upper panel shows the colour image processed as in Figure 2, and the lower panel shows a grey scale of the corresponding raw data overlaid by solid white circles that identify the positions of peaks with full width at half maximum in depth of <3 m. The relative colour scale in the upper panel is the same as in Figure 2, but the absolute values have been shifted. In the lower panel, darker shading corresponds to greater lidar return on a logarithmic scale. The white lines in the upper panel outline the half-power points. The black line on the top is a plot of the layer thickness, with 3 m denoted by a horizontal line.

fairly well for layers thicker than the pulse length, but the relative error can be large for layers thinner than 1 m. An error of one sample (11 cm) in the measured thickness results in an uncertainty in the estimated layer thickness of ~12 cm when the actual thickness is 3 m. For thinner layers, the uncertainty is greater: 18 cm for a layer 1 m thick and 25 cm for a layer 0.7 m thick. Narrow peaks were identified as those where the corrected thickness was <3 m; peaks >3 m were not considered to be thin to this study.

(vi) Then, the image of each original data file was displayed on a computer screen with the positions of the narrow peaks superimposed. Continuous layers were identified manually as regions where the individual narrow peak positions were tightly clustered along a line. Scattered narrow peaks were also observed in the data, but were not selected. Many of those were near the depth limit of the lidar and were caused by system noise spikes. The difference between a continuous layer and scattered individual peaks was generally very clear to the eye, as seen in the example of Figure 4. In the bottom half of that figure, continuous thin layers are evident as the line of circles between 1660 and 2590 m, with gaps at 2000 and 2250 m, and the line between 3660 and 5210 m, with gaps at 4670 and 4810 m. Scattered circles between 3000 and 3800 m represent a few thinner segments of a generally thicker layer. Near the detection limit of the lidar (<20 m in this example), most of the scattered narrow peaks can be attributed to system noise spikes.

(vii) Finally, the length, depth, and thickness of each layer were measured. The prevalence of thin layers was estimated as the ratio of the total length of all thin layers in a given region to the total length of flight tracks in that region. The lengths of thin layers at multiple depths at any one location were added together to estimate total length. The prevalence of thin layers was compared with the intensity of stratification in the upper 50 m of the water column. This intensity of stratification was based on the average total density difference between the surface and a depth of 50 m, measured by conductivity–temperature–depth sensor (CTD) casts taken within 20 km of the flight track. Although ideally one would wish to compare the prevalence of the observed thin layers with density gradients measured simultaneously in the water column directly below the aircraft, this was not possible given the difference in ship and aircraft speeds, the large internal wave fields in many of the areas sampled, and the primary focus of the ships on confirming the fish stock estimates of the airborne lidar.

Results

Wind-driven upwelling regions

The Northeast Pacific Ocean along the coast of Oregon and Washington had the greatest concentration of thin layers of any region sampled. Five long transects (Figure 5) were flown out and back during daylight and again after dark on 9 (44°N), 10 (45°N), 11 (46°N), 13 (47°N), and 16 (48°N) July 2003. The period before the start of these flights was characterized by strong upwelling, with average values for the first 7 days in July of 76 $m^3 s^{-1}$ per 100 m of coastline at 45°N and 34 $m^3 s^{-1}$ per 100 m of coastline at 48°N (http://www.pfeg.noaa.gov/products/PFEL/modeled/indices/upwelling/upwelling.html). There was a period of small or negative upwelling indices during the flights. Sea surface temperature (SST) data measured with an infrared radiometer on the aircraft showed a large (4°C)

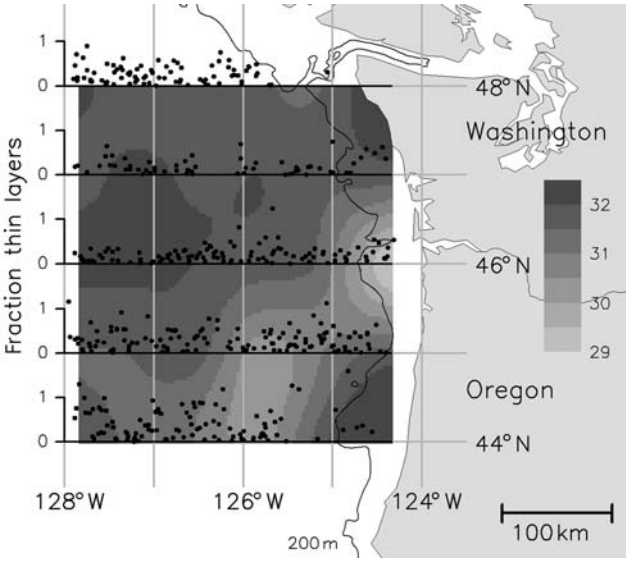

Figure 5. Plots of thin layer prevalence for 6 km segments along the five transects (44–48°N) off Oregon and Washington. Surface salinity contours (psu) show the fresher Columbia River plume to the southwest of the river mouth at the border between Oregon and Washington.

temperature difference between cold nearshore water and warmer water offshore along 44°N. No such pattern was observed along the other lines. SST data from satellite on 9 July suggest that this was a real spatial pattern, and not an effect of warming of the nearshore water during the 8 days over which the series of flights was made. This pattern is typical of an upwelling relaxation event, with persistent upwelling at a hotspot, which is common in the region.

The oceanography of the region is also strongly influenced by fresh-water input, as can be seen in Figure 5. The plume from the Columbia River (the border between Oregon and Washington) extends from the mouth of the river southwest through the study area, as is typical during periods of upwelling. These surface salinity values, taken from CTD casts made on the same day as the corresponding flights, correlate well ($r^2 = 0.87$) with the overall density change in the upper 50 m. The average value of this density change was quite large (1.9 kg m^{-3}), with a value at the mouth of the river reaching 4.5 kg m^{-3}.

Thin layers were prevalent throughout the region in deep-water offshore environments as well as over the continental slope and shelf (Figure 5). They were also prevalent in regions influenced by interactions between upwelling and the Columbia River plume, as well as in areas far from the influence of fresh-water inputs (Figure 5). In fact, the only two areas where thin layers were less prevalent were the shelf waters off northern Washington (48°N east of 125.6°W) and the waters inshore of the Columbia River plume in southern Oregon (44°N east of 125.5°W).

In total, data were analysed from >8000 km of track line, about evenly divided between day and night. The overall prevalence of thin layers was 19% by day and 6% at night. The average depth was 9.5 m by day and 12.9 m at night, and the average thickness was 2.2 m by day or night. Multiple thin layers were common (Figure 2b). Such multiple thin layers contributed to the larger values of the prevalence index (Figure 5) and were the sole cause of index values >1. The fraction of the layer area with multiple layers was 10.5% by day and 2.7% at night. Even three layers were occasionally observed (0.65% of the thin layers by day and 0.16% at night). Layers in this region showed a variety of patterns of spatial variation ranging from layers with uniform intensity and thickness to highly variable layers that included thicker regions and holes (Figures 2a and b and 4).

The total coverage by thin layers observed on the outbound leg of each of the long transects in Figure 5 was well correlated ($r^2 = 0.71$) with that observed on the inbound leg. This suggests that the large-scale conditions for thin layers were not changing on the 1–2 h time-scale of these flights. The correlation between the day and night values (averaged over outbound and inbound legs) was even higher ($r^2 = 0.94$), although fewer layers were observed at night than by day.

There was a moderate correlation between the average of the backscattering strength of those layers within 20 km of each CTD cast and surface salinity ($r^2 = 0.44$), and with the overall density difference between the surface and a depth of 50 m ($r^2 = 0.50$). The correlations were largely determined by the very strong layers [$\beta(\pi) = 5.7 \times 10^{-5}$ m^{-1} sr^{-1}] at the mouth of the Columbia River. Otherwise, the layer strengths were generally weaker to the south of the river than to the north, with the largest values [up to $\beta(\pi) = 7.1 \times 10^{-6}$ m^{-1} sr^{-1}] along the 48th parallel. The timing of the flights may have been a factor—the flights to the south were made 2 and 3 d after the end of the upwelling event on 7 July, whereas the flights to the north were made 6 and 9 d after the end of the event, so giving plankton layers more time to intensify.

In 1998, 5000 km of lidar measurements were made off the west coast of Spain and Portugal and in the Bay of Biscay north of Spain, ~24% of these at night. By day, there were thin layers in ~1.4% of the area, at night ~3.8%. The average depth was 8.1 m by day and 8.9 m at night. The average thickness was less than observed elsewhere—1.7 m by day and 1.8 m at night. Almost all the observed layers were in the upwelling area off the coast of Portugal. Those flights were made during an upwelling relaxation event that followed a month-long period of strong upwelling. Only daytime flights were made in this area, but layers were observed in 3.8% of the sampled region. The average depth was 8.2 m, and the average thickness was 1.7 m. The layers were very strong (Figure 2c) compared with other layers observed in the region. As shown in Figure 2c, there was a large variability in the depth of thin layers in the region, yet they remained continuous over multi-kilometre scales. Estimates of volume backscatter coefficient are not available, however, because the lidar was not calibrated.

Another wind-driven upwelling system, off the coast of southern California, was sampled between 30 March and 21 April 1997. The tracks covered a little more than 6000 km by day and a little less than this at night. During most of the period, the area was subject to strong northwest winds, leading to strong upwelling. Winds as strong as 15 m s^{-1} were recorded during the April 1997 California Cooperative Fisheries Investigation (CalCOFI) cruise (http://www.calcofi.org). Hydrographic data from the same cruise (http://www.calcofi.org) show little evidence of stratification. The average density difference between the surface and 50 m over all the CalCOFI stations was only 0.38 kg m^{-3}. The greatest density difference was 1.18 kg m^{-3}. Values for stations on the outer half of the lines were generally very small (<0.1 kg m^{-3}). Only a handful of layers were observed: 0.05% of the track by day and 0.02% at night. All were within 10 km of the coast, and all were observed during a relatively quiet period before the strong upwelling event.

Topographic upwelling regions

Flights over the Gulf of Alaska occurred during the periods 20 July–10 September 2001, 11–25 May 2002, 16 July–1 September 2002, and 20 July–2 August 2003. The northern Gulf of Alaska is predominantly a downwelling system, but it still supports a productive ecosystem (Stabeno *et al.*, 2004). In the region around Kodiak Island, the Alaska Coastal Current crosses several canyons in the continental shelf. The interaction of the tides and this current with the canyons and the shallow banks between them mixes nutrients into the euphotic zone. During the periods of the flights, there was also a large fresh-water input into the eastern part of the region, which was carried west by the same current.

In 2001, thin layers were observed in 1.6% of the daytime data and 0.19% of the night-time data near Kodiak Island. The average daytime depth was 5.5 m, and the average night-time depth was 6.5 m. The average thickness was about the same by day and night: 2.1 and 2.0 m, respectively. Multiple thin layers were rarely observed. However, layers in this region (Figure 2d) were remarkably similar to those observed off Oregon (Figures 2a and b and 4) and Iberia (Figure 2c). As illustrated in Figure 2d, thin layers in the region exhibited great variability in depth, yet remained continuous over multi-kilometre scales, much like those seen off Portugal. This particular thin layer was well downstream of the region of topographic upwelling, which indicates that thin layers can occur in regions where wind-driven upwelling is replaced by upwelling of nutrients generated by current flow over topography. The mixing generated by flow around the complex topography is likely to inhibit the formation of strong, persistent gradients in very nearshore waters, but there are large fresh-water inflows into this area that help re-stratify the water column downstream of the mixing areas. In 2002, thin layers were a little more prevalent in this region: 2.5% by day and 0.3% at night. The average depth was ~0.4 m less in 2002 than in 2001, day or night. The average thickness was about the same in both years.

A storm came through the area between 18 and 23 August 2001, and it is interesting to compare the situation around Kodiak Island before and after the storm. The CTD data show a deepening of the mixed layer, from an average value of 12 m before the storm to 15 m thereafter. The lidar data show more thin layers before the storm than after: from 1.8 to 0.31% by day and from 0.22 to 0.04% at night. The depth of the observed layers actually decreases, from 5.8 to 4.8 m by day and from 6.7 to 4.0 m at night.

The region south of the Alaska Peninsula is also a region with topographic upwelling near the shore. In 2003, very few layers (0.4%) were observed offshore there. Many more (14%) were observed closer to shore. The nearshore layers were closer to the surface (9.3 m) than those farther offshore (13.5 m), and they were slightly stronger (5.7×10^{-6} vs. $2.9 \times 10^{-6}\,\mathrm{m^{-1}\,sr^{-1}}$). There was a moderate level of thin layers (5.5%) in this region in 2002, where the flight tracks were midway between the nearshore and offshore tracks of 2003.

In 2002, ~8000 km were flown by day over the Norwegian Sea. During most of the period, the weather was determined by weak low pressure to the west and generally moderate winds. Water density gradients were also generally moderate, with an average difference between the value of the density at a depth of 50 m and at the surface of 1.7 $\mathrm{kg\,m^{-3}}$. Almost all values were between 1 and 2 $\mathrm{kg\,m^{-3}}$, except near the southern coast of Norway. There, fresher water at the surface produced greater differences.

The prevalence of thin layers in these data was low (0.22%), with no layers of any thickness detected in much of the western part of the Norwegian Sea. Most of the thin layers that were observed were within a broad band roughly parallel to the coast from ~64°N to ~67°N. The average depth was 11.2 m, and the average thickness was 2.1 m. The region where thin layers were observed lies roughly along the eastern edge of the 1400 m deep Vøring Plateau, which may affect layer formation through its effects on the Norwegian Atlantic Current (Nilsen and Falck, 2006). Figure 2e, an example of the layers in this region, demonstrates large variations in both depth and thickness, with many layers that do not qualify as thin. This appears to be another case where thin layers are found in regions where interactions between currents and topography create upwelling or other associated conditions favourable to thin-layer formation.

Warm-core eddies

A flight across the Gulf of Alaska on 1 August 2003 passed over a warm-core eddy identified in images of sea surface height, SST, and ocean colour from satellite instruments. This flight was made the day after the 31 July satellite altimeter measurement, and the contours of surface height anomaly from that measurement are plotted in Figure 6. Most of the thin layers in the centre of the gulf along this flight track were associated with that eddy, which extended from about 144°W to 148°W. The average thin-layer depth was 15.6 m.

Two days previously (a day before the sea surface height measurement), there was a flight over the centre and western edge of another warm-core eddy south of the Alaska Peninsula, also identified in Figure 6. The region near the centre of the eddy contained a series of 6–10 km segments with thin layers separated by bands without any detectable layers. Figure 2f is typical of the layers in this eddy and also of those in the eddy in the central gulf. The average depth of 15.8 m was similar to that observed in the eddy in the central gulf. The region along the western edge of the eddy showed no such thin layers. In summary, there were thin layers in 12% of the 200 km of the survey that were within the eddy, and none in the 250 km of the survey that was outside of the main core of the eddy, but still off the continental shelf.

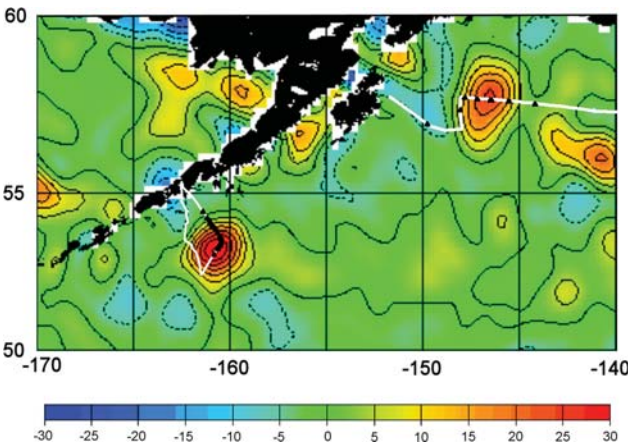

Figure 6. Map of the sea surface height anomaly (cm), the two flight tracks through eddies (white lines), and the locations of the offshore thin layers (black triangles).

Semi-enclosed waters

Observations in semi-enclosed regions of Alaska and British Columbia revealed thin layers with very different characteristics from those off Spain. In the former, the influx of fresh water was very large. This produced strong stratification and high productivity. Conversely, the inlets of northwestern Spain had little or no fresh-water influx.

In May 2002, there was a high prevalence (10%) of thin layers in Prince William Sound, AK. Those layers were highly correlated with zooplankton layers composed largely of calanoid copepods of the genus *Neocalanus* (Churnside and Thorne, 2005). In July of the next year, no measurements were made in the sound, but there was a very high prevalence (19%) in the northern Gulf of Alaska near the mouth of the sound. The layers within the sound were shallower (6.3 vs. 9.1 m) and weaker (3.0×10^{-5} vs. 6.9×10^{-6} m^{-1} sr^{-1}) than those outside. A similar pattern was observed around the Queen Charlotte Islands in 2003. Shallow (6.7 m), strong (5.8×10^{-6} m^{-1} sr^{-1}) layers occurred in the semi-enclosed waters to the east of the islands and deeper (16 m), weaker (2.3×10^{-6} m^{-1} sr^{-1}) layers in the open waters to the west. The layers in the two regions looked similar, except that the depths were different. This pattern is consistent with a strong surface layer of fresher water inside the islands that mixed down as it moved into the open waters offshore.

A very different pattern was observed in the inlets of northwestern Spain, which received very little fresh-water influx at the time of the flights in late summer. Only at night did thin layers appear, covering 3.4% of the flight track at an average depth of 3.8 m and an average thickness of 1.7 m. These layers did not exhibit the depth variability found in almost all the layers observed in other regions; they were very nearly parallel to the surface. *In situ* measurements suggest that the layers were not plankton, but juvenile (age group 0) sardine (*Sardina pilchardus*) that schooled by day, but formed epipelagic layers at night (Uriarte *et al.*, 2002). Therefore, the depth was likely determined by illumination level, rather than density.

Discussion

Patterns of occurrence

Our results demonstrate that thin optical scattering layers are sufficiently intense to be easily detected by NOAA's existing airborne fish lidar. More than 2000 km of optically thin layers were identified in ~80 000 km of flight tracks. These thin layers were observed in a wide variety of ocean environments, ranging from fjords and nearshore waters to deep waters well off the shelf and far from the influences of coastal processes. For example, thin layers were seen in the deep waters of the Eastern Pacific off Oregon and Washington, the Gulf of Alaska, and the Norwegian Sea, as well as in the shelf waters off Oregon, Washington, Alaska, Norway, and Portugal. Furthermore, thin layers were observed in a variety of physical environments ranging from the wind-driven upwelling environments off the west coasts Oregon, Washington, and Portugal to regions where winds are normally unfavourable for upwelling, such as the waters of the Gulf of Alaska. They were also found in regions with little fresh-water inflow as well as in regions with large local fresh-water inflows. The results clearly indicate the value of lidar for rapidly collecting the spatial datasets needed for addressing phenomenological questions about whether thin layers can occur in a region or under a set of forcing conditions. A summary of the prevalence of thin layers by location, time, and expected oceanographic mechanism is presented in Table 1.

Although thin layers can occur in most areas, their frequency of occurrence, intensity, and spatial extent varied dramatically. For example, frequency of occurrence ranged from highs of 20% in some areas (such as areas off Oregon and Washington during upwelling relaxation events) to frequencies of well below 1% in other areas (such as in the Norwegian Sea and the Southern California Bight). It is very evident from the data that while some of these differences are probably reflections of absolute regional difference in the ability of a system to support thin layers, in other cases it almost certainly reflects the environmental conditions at the time of the lidar surveys. For example, the differences seen between the waters off the US Pacific Northwest and the California Bight are almost certainly a reflection of the fact that intense local winds off California were suppressing thin layers at the time of the survey, whereas the upwelling relaxation conditions off the Pacific Northwest were favourable for thin-layer development at the time of that study. This is even more evident in those cases where thin layers detected before storms were not detected in subsequent flights during or after the storm (see below). These results should not be surprising because they are completely consistent with time-series field observations (Dekshenieks *et al.*, 2001; Sullivan *et al.*, 2005) and models of the thin-layer mechanisms (Donaghay and Osborn, 1997).

Table 1. Summary of thin layer observations.

Location	Time	Mechanism	Prevalence
NE Pacific (Oregon, Washington)	July 2003	Wind-driven upwelling, fresh-water inflow	High (19% day, 6% night)
Eastern Atlantic (Portugal)	August – September 1998	Wind-driven upwelling	Moderate (3.8%)
California Bight	April 1997	Wind-driven upwelling	Low (0.02 – 0.05%)
Western Alaska	May 2002, July 2003	Topographic upwelling	High (5.5 – 14%)
Gulf of Alaska (Kodiak Island)	July – September 2001, May – September 2002	Topographic upwelling	Moderate (1.6 – 2.5%)
Norwegian Sea	July 2002	Topographic upwelling	Low (0.2%)
Central Gulf of Alaska	May 2002, July 2003	Warm-core eddy	Moderate (2.0 – 6.6%)
Western Alaska	July 2003	Warm-core eddy	Moderate (3.1%)
Eastern Atlantic (Spain)	August/September 1998	Light level	Moderate (0 – 0.4% day, 3.4 – 4.1% night)
Northern Gulf of Alaska	May 2002, July 2003	Fresh-water inflow	High (10 – 19%)
Eastern Gulf of Alaska	September 2001, May 2002, July 2003	Fresh-water inflow	Moderate (1.4 – 5.8%)

Spatial continuity of thin layers: patterns and implications

Three distinctly different spatial patterns of continuity were evident in the lidar data. Each is discussed in sequence below.

Class 1

These thin layers were consistently <3–4 m thick, extended over kilometres, and showed spatial continuity over their entire length. For example, the thin layer seen off Portugal (Figure 2c) was spatially continuous for nearly 10 km, and that seen in the Gulf of Alaska south of Kodiak Island (Figure 2d) was spatially continuous for nearly 2 km. This class of layer had no thickened regions (as did Class 2) and no regions where the layer became too thin or too weak to be detected by the lidar (as did Class 3). Such spatially continuous structures are consistent with the idea that episodic shear events can spread plankton patches into continuous thin layers covering multiple kilometres (Donaghay and Osborn, 1997; Osborn, 1998). Such layers can also be generated behaviourally when plankton aggregate along a continuous large-scale feature such as a nutricline (PLD, unpublished data). The spatial continuity (lack of gaps) of such thin layers suggests that localized vertical mixing events (from shear instabilities and breaking internal waves, for example) did not occur over the length scale of the thin layer during its development.

Class 2

These thin layers were clearly parts of much longer layers that had both regions that qualified as thin layers and regions where the layer became more intense and much thicker than the 3-m criterion. For example, the thin layers illustrated in Figures 2a and 4 (from deep water off Oregon) were clearly parts of a larger scale structure that also contained thicker regions of high backscatter. The pattern is consistent with what we might be expect to see if episodic increases in current shear spread a series of plankton patches into thin layers (Donaghay and Osborn, 1997; Osborn, 1998).

Class 3

The Class 3 thin layers appeared to be part of a larger scale structure that was broken into shorter segments by gaps where the layer became too thin or too weak to be detected by the lidar. Good examples of this case are the near-surface thin layers between 1.5 and 2.5 km in Figure 4. The gaps in such layers are consistent with what might be expected along a flight track that crossed a set of filaments, such as those seen with squirts and jets in upwelling areas (Miller *et al.*, 1999; Johnston *et al.*, 2008). Such gaps could also be the result of intense grazing by schools of planktivorous fish. In other cases, these gaps are regions where the layer becomes much less intense but thicker. The pattern is consistent with what we might expect if a thin layer were disrupted by a localized mixing event caused by internal wave breaking (Woods, 1968).

Impact of internal waves on thin-layer depth and thickness

Wave-like vertical displacements were a common feature in many of the thin layers detected by lidar. Two distinct types were observed, with very different impacts on thin-layer thickness. Each of these too is considered below.

First, there were cases where the wave-like variations in depth were much less than the average depth. For example, continuous thin layers on the shelf off Kodiak Island (Figure 2d) and Portugal (Figure 2c, for distance >2 km) varied in depth spatially in a wave-like pattern that was quite consistent with internal wave motions seen in time-series data collected at one location, such as the vertical motions in zooplankton thin layers seen by Holliday *et al.* (1998) using profiling acoustic moorings. Spectral analysis of the depth of the Portugal layer between 2 and 10 km showed that the spectrum was very close to classic Garrett and Munk (1979) internal wave spectra (Figure 7), suggesting perturbation by a linear internal wave field. Such linear waves are a common feature on open coastal shelves (Garrett and Munk, 1979). Although shear generated by such waves has been hypothesized to help generate thin layers (Franks, 1995), no dependence of layer thickness on linear internal wave displacement was observed. Variability of layer thickness seems to depend on other processes, such as turbulence and plankton swimming behaviour.

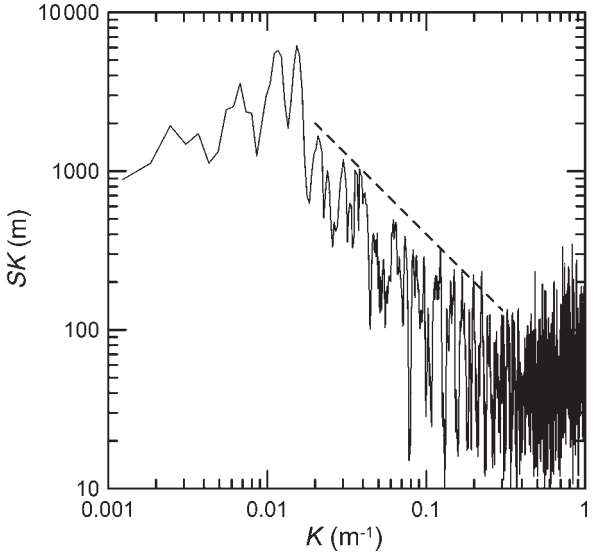

Figure 7. Plot of the product of wave number K and the power spectral density S as a function of K for the depth of the layer in Figure 2c. The dashed line represents the K^{-2} dependence expected for a Garrett and Munk (1979) spectrum.

Second, there were cases where wave-like displacements in layer depth were comparable with the layer depth (Figure 2c, for distance ≈1 km). The best example of this was observed in the centre of the Gulf of Alaska, when the lidar captured a large nonlinear internal wave propagating through the area along the axis of flight (see Churnside and Ostrovsky, 2004, for a full discussion). In that case, the layer thickness varied dramatically in space as the wave caused changes in layer depth. Although the layer was too thick (4–6 m) to meet the 3-m thin-layer criterion at that location (it was "thin" elsewhere along the transect), the results indicate that the large shear generated by non-linear internal waves can stretch plankton layers to generate thin segments embedded in a large-scale, layered structure with much thicker segments. Evidence of this is also seen in Figure 2c, where there is a short decrease in the layer depth near the leading edge of the downward pulse of the wave near 1 km.

Effects of wind-driven upwelling

Thin layers were most frequently observed in upwelling regions during relaxation events following periods of strong upwelling.

This result is consistent with the predictions of biophysical models of thin layers in upwelling areas (Donaghay and Osborn, 1997). Upwelling can have several effects relevant to the formation of thin layers. Active upwelling brings nutrients to the surface, allowing plankton growth and hence the high biomasses inside thin layers that are critical to detection by lidar. Such upwelling can be driven by winds (off Oregon, Washington, and Portugal), topographic interactions with currents (Kodiak Island), and by some types of ocean eddy (McGillicuddy *et al.*, 2007). Upwelling winds can also increase shear that can spread patches into thin layers (Donaghay and Osborn, 1997; Osborn, 1998). However, the strong winds that can create upwelling nutrient-rich waters from depth can also mix the upper water column, thus dissipating existing and preventing the formation of new thin layers near the surface (Donaghay and Osborn, 1997). This would be consistent with the extremely small numbers of thin layers seen off southern California during the intense upwelling winds and deep mixing during the lidar surveys there. Such deep mixing can be suppressed if local vertical density gradients are enhanced by the upwelling process or by strong fresh-water inputs to the upwelling region. This is consistent with the more intense thin layers seen in the Columbia plume areas off Oregon in this study. Temporary relaxation of the upwelling winds can also lead to re-stratification of the upper water column and the development of near-surface thin layers that result from a combination of enhanced *in situ* growth and behavioural aggregation into thin layers by motile plankton (Donaghay and Osborn, 1997). This may be a very important mechanism in generating the intense thin layers seen off Oregon, Washington, and Portugal during upwelling relaxation events sampled during flights in those areas. It is almost certainly responsible for the very-near-surface layers that were evident in the data off Oregon and Washington, but too close to the surface to be included in this analysis.

Effects of topographic upwelling

Current flow over topography can induce upwelling of nutrients into surface waters, so stimulating plankton productivity and biomass (Stabeno *et al.*, 2004). This appears to be an important mechanism in generating the thin layers seen off Kodiak Island (Figure 2d) and those seen along the eastern edge of the 1400 m deep Vøring Plateau in the Norwegian Sea (Figure 2e), where the topography interacts with the Norwegian Atlantic Current (Orvik and Niiler, 2002). Although it is well established that the flow of the Alaska Coastal Current over rough topography south of Kodiak Island generates considerable vertical mixing and an enhanced flux of nutrients in surface water (Stabeno *et al.*, 2004), two factors make it much more difficult to predict where and when thin layers might be in that area. First, the strong currents there can be expected to laterally transport plankton populations substantial distances downstream (westward) during the time it takes the plankton to create sufficient biomass to form thin layers that can be detected by lidar. Second, complex interactions between frequent storms and the variable amount of fresh-water stratification in the area (Stabeno *et al.*, 2004) can be expected to complicate evaluation of the impact of storms on dispersing thin layers of plankton. Given this, it is not surprising that although the lidar surveys revealed several "textbook" thin layers in the area, hence proving that they can be found in this environment (Figure 2d), their pattern of occurrence appeared to vary widely from year to year or even with successive flights within a given year. This is quite different from the situation in wind-driven upwelling systems, where relaxation events allow thin layers to form over large areas.

Impact of eddies on thin-layer formation

One of the exciting discoveries in this study was that thin layers in the Gulf of Alaska were associated with eddies near the shelf south of the Alaska Coastal Current (Figures 2f and 6). This discovery is important for two reasons. First, it helps support the idea that these eddies operate as traps that minimize lateral dispersion, so giving plankton (and fish larva) populations time to convert nutrients into plankton biomass and transfer that up through the food chain to fish larvae. This idea is well established in the fish literature (Sinclair, 1988), but it has been proposed here as a mechanism for thin layer formation. Second, it suggests that the circulation and vertical physical structure within these eddies reduces vertical mixing, so allowing thin layers to develop and persist. This is a whole new mechanism that needs to be further explored. Third, it helps provide additional evidence of Lasker's (1975) hypothesis that thin-layer formation may be critical to fish larva success by providing a highly concentrated food resource during critical stages of development. For example, the results suggest that being trapped in one of these eddies not only allows fish larvae to exploit the enhanced food resources generated by nutrients injected by topographic upwelling, but it also allows them to find and exploit locally enhanced concentrations of prey found in the thin layers. This could be a huge advantage in a highly dispersive system like the Gulf of Alaska where winds tend to induce downwelling rather than upwelling (Stabeno *et al.*, 2004).

Detection and characterization of thin layers using lidar vs. *in situ* optics

The definition of a thin layer used here is somewhat different from that used for defining thin layers using *in situ* optical data, e.g. measurements of the vertical structure of inherent optical properties (IOPs) such as absorption, attenuation, fluorescence, or backscatter. This difference in approach is necessitated both by the inherent differences in the properties being measured (a spatial series of nearly instantaneous profiles of lidar backscatter vs. vertical profiles of IOPs collected over some interval of time and space) and the vertical integration of each individual measurement (centimetre scale for IOPs vs. decimetre plus vertical scales for lidar). The nearly instantaneous nature of the lidar profiles means that sequential profiles can be used to identify where the vertical structure has sufficient lateral (or temporal) continuity to qualify as a thin layer. In contrast, the 15–30 min delay between typical IOP profiles requires the application of two secondary criteria to ensure that one is detecting a temporally/spatially continuous thin layer rather than a micro-patch with lateral scales of less than a few metres. For example, Dekshenieks *et al.* (2001) found that features <3.6 m thick were not temporally/spatially continuous (and hence "thin layers") unless they contained more than six data points and had a peak height of three times that of the surrounding water.

Future directions

Although the lidar was successful in identifying thin layers according to the definition used here, the current configuration is not capable of resolving layers that are thinner than $\sim$1 m. It also tends to overestimate the thickness of layers that are tilted relative to the illumination or are not flat within the illuminated area. As a

result, the lidar configuration used in this study underestimates the occurrence of layers thinner than 1 m and probably underestimates the amplitude of the volume backscatter of layers that have narrow peaks. Two modifications would allow resolution of layers down to 10–20 cm, so providing estimates of layer occurrence and structure that are comparable with the best *in situ* methods. The first would be to shorten the laser pulse length from the current value of about 12 to 1 ns. This would provide a resolution in water of about 10 cm. The second would be to narrow the beam divergence and the field of view of the receiver. Narrowing the field of view to ~1.7 m radius would produce a 10-cm depth difference across the beam for a 15° incidence angle. An incidence angle closer to nadir would allow a wider beam to obtain the same effect.

Another improvement for thin-layer surveys would be the addition of a second receiver channel to obtain the depolarization ratio. This would aid in identification of the type of scattering particle present. This would be particularly interesting for scattering layers at the surface, because bubbles would very nearly preserve polarization, whereas particles with non-spherical geometries, such as plankton, would tend to depolarize the scattered light.

Although airborne lidar can characterize the spatial characteristics of thin scattering layers over scales that are not possible with *in situ* measurements, the composition of those layers is unknown. Intercomparison of lidar and *in situ* measurements should be done to allow identification of the lidar signatures of different scattering types (i.e. bubbles, sediments, phytoplankton, and zooplankton) to the extent possible. Even with this information, a complete understanding of thin layers will require *in situ* measurements of the detailed properties at selected locations. For example, Table 1 suggests that the likely mechanism for the observed thin layers off Spain was a behavioural response to light level. This was a reasonable conjecture based on the diurnal pattern, but *in situ* sampling was required to understand what the organisms were and their behaviour.

Acknowledgements

This analysis was partially supported by the Office of Naval Research Optics and Biology Program under Award Numbers N0001404IP20075 (JHC) and N000140410276 (PLD). The 2003 CTD data from the NE Pacific were provided by Dave Griffith of the NOAA Southwest Fisheries Science Center, the 2001 and 2002 CTD data from the area around Kodiak Island by Mike Guttormsen of the NOAA Alaska Fisheries Science Center, and the CTD data from the Norwegian Sea by Eirik Tenningen of the Norwegian Institute of Marine Research. Bill Pichel of the NOAA National Environmental Satellite and Information Service provided the satellite altimeter map. Jim Wilson of ESRL was the chief engineer for Fish Lidar during the entire period covered in this paper. Funding to pay the Open Access publication charges for this article was provided by the NOAA Science and Technology Infusion Program.

References

Alldredge, A. L., Cowles, T. J., MacIntyre, S., Rines, J. E. B., Donaghay, P. L., Greenlaw, C. F., Holliday, D. V., *et al.* 2002. Occurrence and mechanisms of formation of a dramatic thin layer of marine snow in a shallow Pacific fjord. Marine Ecology Progress Series, 233: 1–12.

ANSI. 1993. Safe Use of Lasers, Standard Z-136.1. American National Standards Institute, New York. 120 pp.

Bjornsen, P. K., and Nielsen, T. G. 1991. Decimetre scale heterogeneity in plankton during a pycnocline bloom of *Gyrodinium aureolum*. Marine Ecology Progress Series, 73: 263–267.

Brown, E. D., Churnside, J. H., Collins, R. L., Veenstra, T., Wilson, J. J., and Abnett, K. 2002. Remote sensing of capelin and other biological features in the North Pacific using lidar and video technology. ICES Journal of Marine Science, 59: 1120–1130.

Carrera, P., Churnside, J. H., Boyra, G., Marques, V., Scalabrin, C., and Uriarte, A. 2006. Comparison of airborne lidar with echosounders: a case study in the coastal Atlantic waters of southern Europe. ICES Journal of Marine Science, 63: 1736–1750.

Cassie, R. M. 1963. Microdistribution of plankton. Oceanography and Marine Biology: an Annual Review, 1: 223–252.

Churnside, J. H., Demer, D. A., and Mahmoudi, B. 2003. A comparison of lidar and echosounder measurements of fish schools in the Gulf of Mexico. ICES Journal of Marine Science, 60: 147–154.

Churnside, J. H., and Ostrovsky, L. A. 2004. Lidar observation of a strongly nonlinear internal wave train in the Gulf of Alaska. International Journal of Remote Sensing, 26: 167–177.

Churnside, J. H., and Thorne, R. E. 2005. Comparison of airborne lidar measurements with 420 kHz echo-sounder measurements of zooplankton. Applied Optics, 44: 5504–5511.

Churnside, J. H., Wilson, J. J., and Tatarskii, V. V. 1997. Lidar profiles of fish schools. Applied Optics, 36: 6011–6020.

Churnside, J. H., Wilson, J. J., and Tatarskii, V. V. 2001. Airborne lidar for fisheries applications. Optical Engineering, 40: 406–414.

Cowles, T. J., Desiderio, R. A., and Carr, E. 1998. Small-scale planktonic structure: persistence and trophic consequences. Oceanography, 11: 4–9.

Dekshenieks, M. M., Donaghay, P. L., Sullivan, J. M., Rines, J. E. B., Osborn, T. R., and Twadowski, M. S. 2001. Temporal and spatial occurrence of thin phytoplankton layers in relation to physical processes. Marine Ecology Progress Series, 223: 61–71.

Donaghay, P. L. 2004. Critical scales for understanding the structure, dynamics, and impacts of zooplankton patches. Journal of the Acoustical Society of America, 115: 2520.

Donaghay, P. L., and Osborn, T. R. 1997. Toward a theory of biological–physical control of harmful algal bloom dynamics and impacts. Limnology and Oceanography, 42: 1283–1296.

Donaghay, P. L., Rines, H. M., and Sieburth, J. M. 1992. Simultaneous sampling of fine scale biological, chemical, and physical structure in stratified waters. Ergebnisse der Limnologie ERLIA6, 36: 97–108.

Franks, P. J. S. 1995. Thin layers of phytoplankton: a model of formation by near-inertial wave shear. Deep Sea Research I, 42: 75–83.

Garrett, C., and Munk, W. 1979. Internal waves in the ocean. Annual Reviews of Fluid Mechanics, 11: 339–369.

Gordon, H. R. 1982. Interpretation of airborne oceanic lidar: effects of multiple scattering. Applied Optics, 21: 2996–3001.

Hanson, A. K., and Donaghay, P. L. 1998. Micro- to fine-scale chemical gradients and layers in stratified coastal waters. Oceanography, 11: 10–17.

Hoge, F. E., Wright, C. W., Krabill, W. B., Buntzen, R. R., Gilbert, G. D., Swift, R. N., Yungel, J. K., *et al.* 1988. Airborne lidar detection of subsurface oceanic scattering layers. Applied Optics, 27: 3969–3977.

Holliday, D. V., Donaghay, P. L., Greenlaw, C. F., McGehee, D. E., McManus, M. M., Sullivan, J. M., and Miksis, J. L. 2003. Advances in defining fine- and micro-scale pattern in marine plankton. Aquatic Living Resources, 16: 131–136.

Holliday, D. V., Pieper, R. E., Greenlaw, C. F., and Dawson, J. K. 1998. Acoustic sensing of small-scale vertical structures in zooplankton assemblages. Oceanography, 11: 18–23.

Johnson, P. W., Donaghay, P. L., Small, E. B., and Sieburth, J. McN. 1995. Ultrastructure and ecology of *Perispira ovum* (Ciliophora: Litostomatea): an aerobic, planktonic ciliate that sequesters the

chloroplasts, mitochondria, and paramylon of *Euglena proxima* in a micro-oxic habitat. Journal of Eukaryotic Microbiology, 42: 323–335.

Johnston, T. M., Cheriton, O. M., Pennington, J. T., and Chavez, F. P. 2008. Thin phytoplankton layer formation at eddies, filaments, and fronts in a coastal upwelling zone. Deep Sea Research II, doi:10.1016/j.dsr2.2008.08.006.

Lasker, R. 1975. Field criteria for survival of anchovy larvae: the relation between inshore chlorophyll maximum layers and successful first feeding. Fishery Bulletin US, 73: 453–462.

Lewis, G. D., Jordan, D. L., and Roberts, P. J. 1999. Backscattering target detection in a turbid medium by polarization discrimination. Applied Optics, 38: 3937–3944.

Mason, R. P., Fitzgerald, W. F., Donaghay, P. L., and Sieburth, J. M. 1993. Mercury speciation and cycling in the Pettaquamscutt Estuary. Limnology and Oceanography, 36: 1227–1241.

McGillicuddy, D. J., Anderson, L. A., Bates, N. R., Bibby, T., Buesseler, K. O., Carlson, C. A., Davis, C. S., *et al.* 2007. Eddy/wind interactions stimulate extraordinary mid-ocean plankton blooms. Science, 316: 1021–1026.

McManus, M. A., Alldredge, A. L., Barnard, A. H., Boss, E., Case, J. F., Cowles, T. J., Donaghay, P. L., *et al.* 2003. Characteristics, distribution and persistence of thin layers over a 48-hour period. Marine Ecology Progress Series, 261: 1–19.

McManus, M. A., Cheriton, O. M., Drake, P. J., Holliday, D. V., Storlazzi, C. D., Donaghay, P. L., and Greenlaw, C. F. 2005. Effects of physical processes on structure and transport of thin zooplankton layers in the coastal ocean. Marine Ecology Progress Series, 301: 199–215.

Miller, A. J., McWilliams, J. C., Schneider, N., Allen, J. S., Barth, J. A., Beardsley, R. C., Chavez, F. P., *et al.* 1999. Observing and modeling the California Current System. EOS Transactions of the American Geophysical Union, 80: 533–539.

Mullin, M. M., and Brooks, E. R. 1976. Some consequences of distributional heterogeneity of phytoplankton and zooplankton. Limnology and Oceanography, 21: 784–796.

Nielsen, T. G., Kiørboe, T., and Bjørnsen, P. K. 1990. Effects of a *Chrysochromulina polylepis* subsurface bloom on the planktonic community. Marine Ecology Progress Series, 62: 21–35.

Nilsen, J. E. Ø., and Falck, E. 2006. Variations of mixed layer properties in the Norwegian Sea for the period 1948–1999. Progress in Oceanography, 70: 58–90.

Orvik, K. A., and Niiler, P. 2002. Major pathways of Atlantic water in the northern North Atlantic and Nordic Seas toward Arctic. Geophysical Research Letters, 29: 1896–1899.

Osborn, T. R. 1998. Finestructure, microstructure, and thin layers. Oceanography, 11: 36–43.

Petrenko, A. A., Zaneveld, J. R. V., Pegau, W. S., Barnard, A. H., and Mobley, C. D. 1998. Effects of a thin layer on reflectance and remote-sensing reflectance. Oceanography, 11: 48–50.

Platt, T., and Denman, K. 1975. Spectral analysis in ecology. Annual Review of Ecology and Systematics, 6: 189–210.

Rines, J. E. B., Donaghay, P. L., Dekshenieks, M. M., and Sullivan, J. M. 2002. Thin layers and camouflage: hidden *Pseudonitzschia* spp. (Bacillariophyceae) populations in a fjord in the San Juan Islands, Washington, USA. Marine Ecology Progress Series, 225: 123–137.

Scranton, M. I., Crill, P., de Angelis, M. A., Donaghay, P. L., and Sieburth, J. M. 1993. The importance of episodic events in controlling the flux of methane from anoxic basins. Global Biogeochemical Cycles, 7: 491–507.

Scranton, M. I., Donaghay, P. L., and Sieburth, J. McN. 1995. Nocturnal methane accumulation in the pycnocline of an anoxic estuarine basin. Limnology and Oceanography, 40: 666–672.

Sieburth, J. M., and Donaghay, P. L. 1993. Planktonic methane production and oxidation within the algal maximum of the pycnocline: seasonal fine scale observations in an anoxic estuarine basin. Marine Ecology Progress Series, 100: 3–15.

Sinclair, M. 1988. Marine Populations: an Essay on Population Regulation and Speciation. University of Washington Press, Seattle. 252 pp.

Stabeno, P. J., Bond, N. A., Hermann, A. J., Kachel, N. B., Mordy, C. W., and Overland, J. E. 2004. Meteorology and oceanography of the northern Gulf of Alaska. Continental Shelf Research, 24: 859–897.

Sullivan, J. M., Twardowski, M. S., Donaghay, P. L., and Freeman, S. A. 2005. Use of optical scattering to discriminate particle types in coastal waters. Applied Optics, 44: 1667–1680.

Uriarte, A., Scalabrin, C., Gómez, J. A., Porteiro, C., Pestana, G., and Churnside, J. H. 2002. Experimental surveys for the assessment of juveniles, FAIR CT-3374 final report. Commission of the European Communities. Directorate General for Fisheries DGXIV, Brussels.

Vasilkov, A. P., Goldin, Y. A., Gureev, B. A., Hoge, F. E., Swift, R. N., and Wright, C. W. 2001. Airborne polarized lidar detection of scattering in the ocean. Applied Optics, 40: 4353–4364.

Woods, J. D. 1968. Diurnal behavior of the summer thermocline off Malta. Ocean Dynamics, 21: 106–108.

Zaneveld, R. J. V., and Pegau, W. S. 1998. A model for the reflectance of thin layers, fronts, and internal waves and its inversion. Oceanography, 11: 44–47.

Zorn, H. M., Churnside, J. H., and Oliver, C. W. 2000. Laser safety thresholds for cetaceans and pinnipeds. Marine Mammal Science, 16: 186–200.

doi:10.1093/icesjms/fsp029